INFRARED SPECTRUM OF HYDROGEN FLUORIDE: SHAPES, POSITIONS AND INTENSITIES OF HIGH J LINES IN THE FUNDAMENTAL BAND

L. F. Eldreth and R. J. Lovell

The University of Tennessee
Department of Physics
Knoxville, Tennessee

Contract No. AF19(604)-7981

Project No. 7670

Task No. 767002

Scientific Report No. 3
December 1962

Prepared for

GEOPHYSICS RESEARCH DIRECTORATE
AIR FORCE CAMBRIDGE RESEARCH LABORATORIES
OFFICE OF AEROSPACE RESEARCH
UNITED STATES AIR FORCE
BEDFORD, MASSACHUSETTS

Alvin H. Nielsen, Project Director

Requests for additional copies by agencies of the Department of Defense, their contractors, and other Government agencies, should be directed to the:

Armed Services Technical Information Agency
Arlington Hall Station
Arlington 12, Virginia.

Department of Defense contractors must be established for ASTIA services or have their "need-to-know" certified by the cognizant agency of their project or contract.

All other persons and organizations should apply to the:

U. S. Department of Commer
Office of Technical Services
Washington 25, D. C.

INFRARED SPECTRUM OF HYDROGEN FLUORIDE: SHAPES, POSITIONS AND INTENSITIES OF HIGH J LINES IN THE FUNDAMENTAL BAND

A Thesis

Presented to

the Graduate Council of

The University of Tennessee

In Partial Fulfillment

of the Requirements for the Degree

Master of Science

---

by

Lester F. Eldreth

December 1962

ACKNOWLEDGEMENT

It gives me great pleasure to acknowledge the help and cooperation I have received from many persons during the course of this investigation. My sincere thanks are due to Dr. Robert J. Lovell, who directed this work, and to Dr. Norman M. Gailar for his many valuable suggestions. I am very grateful to Mr. Ray Mink and Lt. Hugo Hardt of The University of Tennessee Physics Department, and to Mr. Van McCombs of The University of Tennessee Computing Center for their assistance in various phases of this work.

The financial help given me by The University of Tennessee Physics Department through a graduate assistantship and research assistantship was most appreciated. The latter was supported by Contract No. AF19(604)-7981 with the Office of Aerospace Research, United States Air Force.

Thanks are also extended to my wife, Margaret, for her moral support during the period of this study.

Lester F. Eldreth

TABLE OF CONTENTS

LIST OF TABLES

LIST OF FIGURES

CHAPTER I

INTRODUCTION

One studies the infrared spectrum of a molecule for many reasons, but to the physicist only two of these are of major importance. They are (1) to learn more about intramolecular forces and (2) to learn more about intermolecular forces.

The first of these involves a study of the line frequencies and intensities at moderate pressure, since they can be considered to be properties of the isolated molecule. By moderate pressures we mean pressures at which collisions are mostly binary. Frequency measurements lead to information about molecular energy levels, potential energy functions, intramolecular distances, and distortions of a molecule with excitation to higher rotational and vibrational energy levels. Intensity measurements lead to information about the derivative of the molecular dipole moment with respect to the internuclear distance, the interaction of the vibrational and rotational energies of a molecule, and the square of the matrix element of the electric dipole moment.

The second of these involves the study of the shape of a spectral line. Since the shape of a spectral line is not just a property of the isolated molecule, a study of this leads to information concerning the long and short range forces, the paths, and the velocities of a molecule engaging in a collision.

CHAPTER I

INTRODUCTION

One studies the infrared spectrum of a molecule for many reasons, but to the physicist only two of these are of major importance. They are (1) to learn more about intramolecular forces and (2) to learn more about intermolecular forces.

The first of these involves a study of the line frequencies and intensities at moderate pressure*, since they can be considered to be properties of the isolated molecule. By moderate pressures we mean pressures at which collisions are mostly binary. Frequency measurements lead to information about molecular energy levels, potential energy functions, intramolecular distances, and distortions of a molecule with excitation to higher rotational and vibrational energy levels. Intensity measurements lead to information about the derivative of the molecular dipole moment with respect to the internuclear distance, the interaction of the vibrational and rotational energies of a molecule, and the square of the matrix element of the electric dipole moment.

The second of these involves the study of the shape of a spectral line. Since the shape of a spectral line is not just a property of the isolated molecule, a study of this leads to information concerning the long and short range forces, the paths, and the velocities of a molecule engaging in a collision.

The aim of this investigation was to determine the line position and true line shape for as many as possible of the high J spectral lines of the hydrogen fluoride fundamental band. There is a great need for accurate measurement of the line position and true line shape of these high J spectral lines, not only for testing existing theories, but also to provide raw material for further theoretical work.

It is observed experimentally that a spectral line is not sharp, but has a frequency spread around an average or center frequency. Thus it is said to possess a breadth. Depending upon their origin, different kinds of line breadths have been distinguished.

They are:

(1) Natural broadening results from the Heisenburg Uncertainty Principle. The width of an energy level giving rise to a spectral line is inversely proportional to the mean life of the level. This gives a negligible value of about 10^{-9} cm.$^{-1}$ for the width of a line.

(2) Doppler broadening results from the shift in frequency that is observed due to the gas molecules having a velocity component in the direction of the radiation. If the molecules of the gas under observation have a Maxwellian distribution of velocities along the direction of the radiation, calculations show the Doppler shift would give a value of about 10^{-3} cm.$^{-1}$ for the width of an HF line at room temperature.

(3) Pressure broadening is due to collisions between molecules and is the most important broadening mechanism for this investigation.

If it is assumed that the collision time is short compared with the time between collisions and if only binary collisions are considered, then the line width of a pressure broadened spectral line is proportional to the pressure at a given temperature.

(4) Statistical broadening is associated with pressures at which collisions other than binary must also be considered. Due to the continual overlapping of molecular fields, the energy levels and spectral lines arising therefrom are said to have a statistical distribution.

In actual practice another type of broadening occurs that has nothing to do with molecular interactions. This is called instrumental broadening, and is due to the spectral lines being scanned with a slit of finite width, and to imperfect optics. These factors cause a line to be more intense in the wings and less intense at the line center than the true line. Corrections for this effect can be made, but the higher the resolving power of the spectrometer the less this correction need be.

The shape of a spectral line is also dependent upon the temperature of the sample. This is apparent from the fact that the populations of the different energy levels which give rise to the spectral lines are temperature dependent. Doppler broadening resulting from the Doppler shift is also dependent upon the temperature, and for HF the ratio of monomer to polymer is highly temperature dependent. In order to hold the temperature dependent variables constant and to eliminate most of the polymer absorption, this entire study was done at a constant temperature of 100°C.

To study spectral line shapes one would like a spectrum which consists of only a few strong lines. The lines should be separated widely enough so that they do not overlap over the regions of pressures, temperatures, and path lengths used. HF fits these requirements better than does any other molecule. In addition, it is a diatomic molecule which makes the theoretical calculations as simple as possible. While the spectroscopic properties of the HF molecule make it ideally suited for the study of spectral line shapes, other characteristics make it less attractive. It is highly reactive, attacking both the windows and the walls of the absorbing cells. In the vapor phase, at one atmosphere pressure and room temperature it is highly polymerized. Some of the polymers absorb in the region of the P branch of the HF fundamental vibrational-rotational band. There are also many strongly absorbing water lines in this region of the spectrum. However, special techniques and equipment have been developed to overcome these obstacles.

The history of the infrared spectrum of hydrogen fluoride prior to 1956 has been well described by Kuipers (1). Since that time, however, HF has been the subject of much research. This is due in part to Kuipers' (1), Smith's (2) and others demonstrating that HF could be properly handled.

Probably the most extensive work on HF since that time has been carried out at The University of Tennessee and at the Oak Ridge National Laboratory. Many of the line positions of the fundamental and first overtone have been measured quite accurately by Herget, et al. (3), who have also determined the true line shape of many of the lines in the

fundamental band. D. F. Smith and his coworkers (2) have studied the effects of polymer absorption and of foreign gas broadening. The most recent work was done by Mason (4) who has measured the line positions of many of the pure rotational lines.

CHAPTER II

EXPERIMENTAL DETAILS

I. THE SPECTROMETER

The high resolution vacuum-grating spectrometer at The University of Tennessee has been fully described by Herndon and Nielsen (5). Herget (3) has described various modifications and additions to the spectrometer that enable one to use it to a greater advantage for the study of spectral line shapes. All data were taken using the following equipment. A Bausch and Lomb replica grating (5 in. x 8 in.) with 15,240 lines ruled per inch was used in first order. A germanium band pass filter passing about 80 per cent of the radiation between 2.0 μ and 2.8 μ was substituted for the prism monochromator. Detection was accomplished with an Eastman Kodak uncooled Ektron lead sulfide detector operating into a 13-cps Perkin-Elmer chopper-amplifier system. A Kenny pump evacuated the tank housing the spectrometer to a pressure of about 40 μ.*

The spectrometer under these conditions is easily capable of resolving lines separated by 0.1 cm.$^{-1}$ at 4000 cm.$^{-1}$.

---

*This description as well as others in this manuscript follows Herget.

II. THE ABSORPTION CELLS

Three absorption cells were used in this work: One with a path of 1.92 cm., shown in Figure 1; another with a path of 9.78 cm., also shown in Figure 1; and the third with a path of 18.14 cm. The longer cell is identical to the 1.92 cm. cell except for body length and is not shown for this reason.

The 9.78 cm. cell was constructed of brass, and the others were constructed of stainless steel. HF reacts to some extent with these metals, but soon forms surface fluorides which prevent further reactions. Either cell can be mounted on a selsyn-driven rack and pinion so that it can be raised from or lowered into the infrared beam from outside the spectrometer tank.

Previous work with HF in this laboratory has shown that sapphire cell windows resist corrosion very well at moderate pressures and temperatures and transmit most of the 2.5 μ radiation without the appearance of "window bands". For this reason sapphire cell windows were chosen for this work. They were sealed to the cells with teflon gaskets as shown in Figure 1.

Originally this experiment was designed to include a study of the temperature dependence of the line shape parameters (α_o and $\Delta\nu'$) for selected spectral lines. Because temperatures beyond the melting point of teflon would be required for this study, it was decided to seal the windows to the cell with metal O'rings. The metal O'rings were stainless steel tubing 0.094 inches in diameter with 0.006 inch

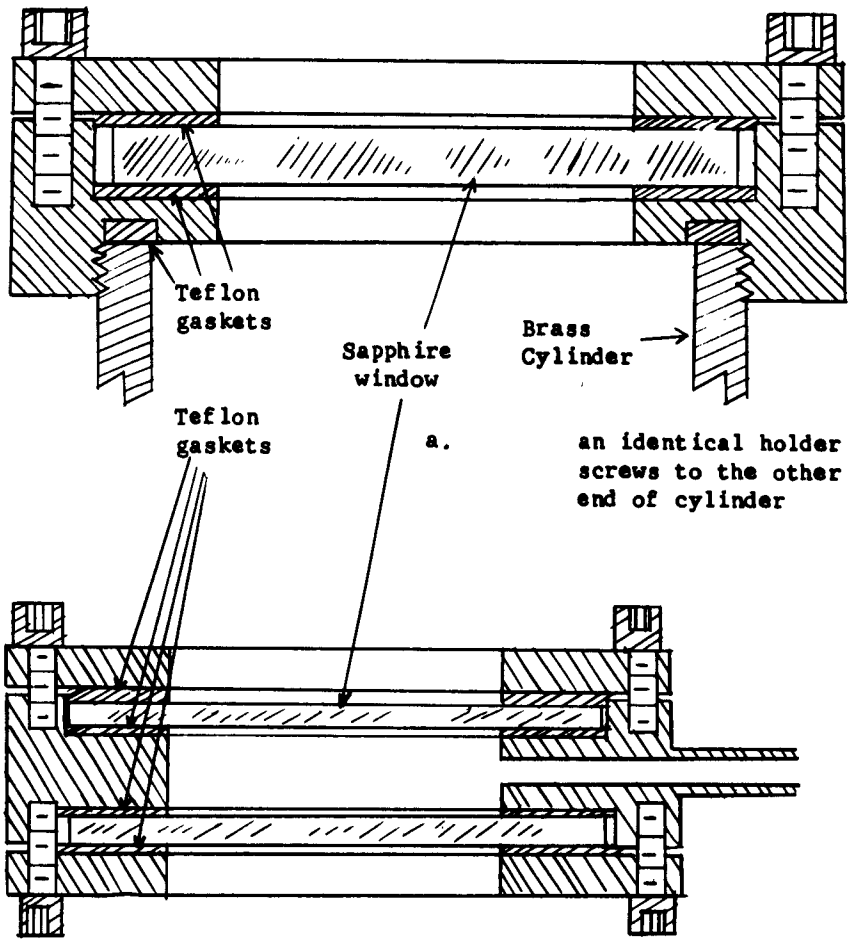

Figure 1. The window holder for the 9.78 cm. cell (a), and the 1.92 cm. cell (b).

walls. They were plated with 0.002 inches of gold and were pressure filled. However, the author using these rings was never able to form an effective seal, so this part of the experiment was abandoned.

III. TEMPERATURE MEASUREMENT

The sample cell was heated by a calrod heating element wrapped around it several times and connected to a variac located outside the spectrometer tank. The manifold and the entire gas handling system were heated with strip heaters and asbestos-covered heating wire. The temperature of the equipment inside the spectrometer tank was measured with a Leeds and Northup thermocouple-potentiometer system. The thermocouple wire was iron-constantan matched by Leeds and Northup to within $\pm$ 0.02°C. The thermocouple leads were attached to the outside of the absorption cell to prevent them from coming in contact with HF.

The following experiment was performed to see if the temperature of the outside of the cell gave an accurate measurement of the temperature of the gas inside the cell.

An iron-constantan thermocouple was attached to the outside of the cell and a copper-constantan thermocouple was placed inside the cell containing one atmosphere of air. The copper-constantan leads were sealed inside the cell with a high temperature wax, and the cell was placed in the spectrometer tank. After the tank was evacuated, the temperatures of the outside of the cell and of the air inside the cell were measured at various temperatures. Table I lists the values obtained by each thermocouple and shows them to be the same within

TABLE I

COMPARISON OF THE TEMPERATURE OF AIR INSIDE THE CELL WITH THE TEMPERATURE OF THE OUTSIDE OF THE CELL BODY

Outside Iron-Constantan		Inside Copper-Constantan	
Millivolt	Temperature (deg. C)	Millivolt	Temperature (deg. C)
0.85	17.0	0.66	17.0
1.15	22.5	0.89	22.9
1.91	37.0	1.43	36.5
2.93	56.5	2.26	55.0
3.91	75.0	3.16	75.4
4.63	88.0	3.68	87.9
5.00	95.0	4.05	95.0
5.23	100.0	4.28	100.0

experimental error. It was concluded from this test that measuring the temperature of the outside of the cell gave an accurate measurement of the temperature of the gas in the cell when the cell was in a vacuum.

IV. PRESSURE MEASUREMENT

Since the entire gas handling system has been described by Herget (3), only the pressure measuring components will be discussed here.

The gas handling system is equipped with a Taylor Differential Pressure Transmitter (Model No. 399RF), a Bourdon gauge, and a Hastings thermocouple gauge. The Taylor Differential Pressure Transmitter accurately measures pressures up to 128 cm. of mercury. The Bourdon gauge has a monel Bourdon tube and is used to measure pressures above 128 cm. of mercury. The Hastings thermocouple gauge is used to measure vacuum.

The spectrometer tank is equipped with a Hastings thermocouple gauge and a vacuum gauge. The vacuum gauge is used for rough measurements.

V. THE METHOD OF CALIBRATION

Since the line positions of most of the HF fundamental lines are accurately known, it was decided to use them as internal standards for calibration purposes.

The frequency of a spectral line, ν (cm.$^{-1}$), is related to the grating constant, K (cm.$^{-1}$), and the angular distance from central image, θ (in degrees) by the equation

$$\nu = \frac{nK}{\sin \theta}$$

where n is the order. In first order, n is unity and the equation becomes

$$\nu = \frac{K}{\sin \theta} \quad .$$

If one knew ν and θ accurately, he could then calculate K. Then, using this value of K and the angular position of some other spectral line, say θ_1, its frequency ν_1 could be determined. Since the spectrometer has two grating drives, this procedure cannot be used. The positioning drive, used to turn the grating to the desired spectral region, is fast but not precise enough to make accurate determinations of the angle θ. The scanning drive, however, is very accurate and thus permits precise angular differences to be measured.

In calibrating in this manner two HF lines are chosen, say R(9) and R(10). Let the frequency of R(9) be called ν_9 and write the grating equation

$$\nu_9 = \frac{K}{\sin \theta}$$

where θ is the angular position of R(9). Then let the frequency of R(10) be called ν_{10} and its angular position be $\theta + \Delta$. The angle Δ is known very accurately. The grating equation for R(10) can be written as

$$\nu_{10} = \frac{K}{\sin(\theta + \Delta)} \quad .$$

Since ν_9 and ν_{10} are known accurately, the two equations can be solved simultaneously for the two unknowns, K and θ. Once these are known accurately, the frequency of any point in the neighborhood of R(9) and R(10) can be determined since the angular distance of the point from θ is accurately known.

As a check on the accuracy of calibrating in this manner, one then calculates the frequency of R(8), using the known values of K and θ and the measured value of Δ. This can be compared with the known value. When this was done, the measured and the known values agreed to within $\pm$ 0.02 $cm.^{-1}$ which is within the limits of experimental error.

Since R(8) is farther removed from the R(9) and R(10) region than R(11), it was felt that this method would also give an accurate measurement of the frequency of R(11). There are two factors which limit the precision of measurement. The first is the result of a slight instrumental drift which limits the reproducibility of the line positions. The second is the inability of the operator to start the recorder and the scanning drive mechanism simultaneously each time.

VI. DETERMINATION OF LINE CENTERS

The chart paper on which the spectral lines are recorded can be calibrated to read angular position directly. Thus the line centers of the spectral lines were determined in the following manner. A number

of points were marked off midway between the sides of a spectral line. Weighting the points near the top the most, a straight line was drawn through these points perpendicular to the edge of the chart paper. This line then gave the angular position of the line center.

On some lines another method was used as a check on the aforementioned procedure. In this method a straight line was drawn up each side of a spectral line and then a straight line was drawn through their intersection perpendicular to the edge of the chart paper. The two methods always agreed to within experimental error.

VII. DETERMINATION OF THE BASE LINE AND ZERO LINE

The method used in determining the base and zero lines in this work is the same as used by Herget (3). These lines must be determined after a spectral line has been recorded before per cent absorption can be determined. The zero line is the position on the chart paper corresponding to zero per cent transmission or 100 per cent absorption, while the base line is the position corresponding to 100 per cent transmission or zero per cent absorption.

The first step in this determination was to scan, with the absorption cell evacuated, the spectral region in which the HF lines of interest happen to lie. This background scan showed the background to be a smooth curve of which small portions could be taken as a straight line. Thus one could determine the base line for lines with no overlap simply by drawing a straight line from one wing to the other.

The zero line is easy to determine for lines that absorb essentially 100 per cent without correction for instrumental broadening. When a line absorbs 100 per cent, there is a flat portion of the spectral line that extends through the line center. Thus the zero line can then be determined by drawing a straight line through this flat portion.

For lines that did not absorb 100 per cent without correction for instrumental broadening, and none of the lines of interest in this study did, determination of the zero line was more difficult. A scan of the HF fundamental region with the slits closed showed the zero line plus stray light to be a straight line on the chart paper for the entire R branch of the HF region, as long as the instrument settings (amplifier controls, glower current, etc.) remained fixed. A second scan with the chopper off showed the stray light to be constant throughout this region. This was expected, since most of the stray light was light that was reflected from the back of the entrance slit and thus did not go through the grating section. As a further check to insure that the zero line on the chart paper was a straight line, the zero line of several HF lines that did absorb 100 per cent with the path length that was used was determined. Since this also showed the zero line to be a straight line, one could then determine the zero line of an HF line that absorbed 100 per cent and use this as the zero line for the HF lines of interest.

The line actually used to determine the zero line was R(4), and it lies approximately 150 $cm.^{-1}$ away from the HF lines of interest on the low wave number side.

It is to be noted that even though a small amount of stray light was present, it did not introduce an error. Since it was present in the base line and in the spectral line, it was subtracted out in determining per cent absorption.

VIII. OVERLAPPING OF SPECTRAL LINES

Most of the spectral lines of interest in this study were run at 4 atmospheres pressure. At this pressure one must consider the possibility of overlap of adjacent lines, since this would influence the determination of the base line. However, a simple calculation shows that overlap of adjacent lines in this region is negligible. This was checked experimentally by comparing the background scan with the scan of the line itself.

IX. CORRECTION FOR INSTRUMENTAL BROADENING

The use of a spectrometer with slits of finite width, imperfect optics, and imperfect alignment results in an observed line shape that is different from the true line shape. The observed line has an increase in absorption in the wings and a decrease in absorption at the line center as compared with the true line shape. This effect is shown in Figure 2. However, far out in the wings of a spectral line where absorption varies slowly with wave number the two shapes are essentially the same, and corrections for instrumental broadening can be neglected.

In order to correct lines broadened in this manner one must first determine the function which describes the line shape that is obtained

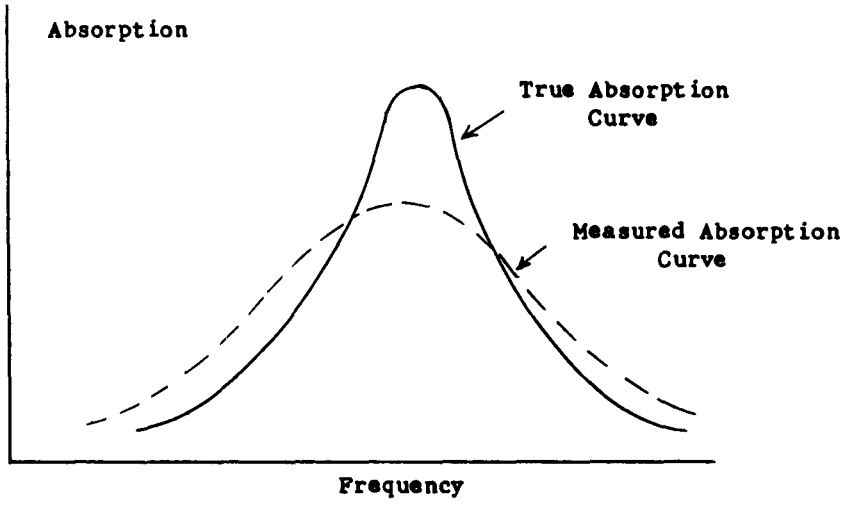

Figure 2. True and measured absorption curves.

when the spectrometer scans a monochromatic line. This function must be normalized to unit intensity, that is, the area under the absorption curve must equal one. This function is called a slit function and is a function of two variables, ν and ν_0, or better ν and $\nu - \nu_0$, where ν_0 is the frequency of the line center, and ν is the frequency of the point of interest on the spectral line.

In actual practice one cannot obtain a monochromatic absorption line, so the method developed by Deeds, et al. (6) was used. Thus this function was determined experimentally by measuring the absorption of a line whose width due to all other causes (such as Doppler, pressure, etc.) was much smaller than the spectral slit width.

It was decided that the R(5) line of the first overtone of CO would be used for this determination. It has approximately the same frequency as the spectral lines of interest in this study and a natural width on the order of 10^{-5} cm.$^{-1}$. This width is completely masked by its Doppler width of about 10^{-3} cm.$^{-1}$ at room temperature. By admitting CO directly into the spectrometer chamber, which provides a path length of about 8.5 meters, adequate absorption was obtained at a pressure of 0.6 cm. of mercury. The line was recorded with a physical slit of 75 microns, which corresponds to a spectral slit of 0.12 cm.$^{-1}$. The line had a half-width at half maximum of 0.07 cm.$^{-1}$. Increasing the CO pressure to 1.0 cm. of mercury did not appreciably increase the measured line width. Thus pressure broadening did not contribute to the line shape, and the Doppler half-width could be used as the true half-width.

The observed shape of the CO line was then normalized to unit area and used as the slit function, $S(\nu - \nu_0, \nu)$. This is shown in Figure 3, and is interpreted as the absorption at frequency ν ($cm.^{-1}$) due to a monochromatic source of frequency ν_0 ($cm.^{-1}$) and of unit intensity when the chief cause of broadening is instrumental. It should be noted that the shape of $S(\nu, \nu_0)$ does not depend on the central frequency ν_0, but instead on the distance from the central frequency, that is, on $(\nu - \nu_0)$. Table II lists the numerical values actually obtained for $S(\nu - \nu_0, \nu)$ at increments of 0.02 $cm.^{-1}$. Each normalized ordinate was obtained by dividing each arbitrary ordinate by the sum of all of the arbitrary ordinates.

The observed absorption $A(\nu)$ in the frequency range ν to $\nu + d\nu$ is related to the true absorption $a(\nu')$ in the frequency range ν' to $\nu' + d\nu'$ by the equation

$$dA(\nu) = S(\nu - \nu', \nu)\, a(\nu')\, d\nu' ,$$

where $S(\nu - \nu', \nu)$ is the value of the slit function at frequency ν'. The computers available at The University of Tennessee cannot handle numerical integration. Because of this, a modification of an approximation method, developed by D. F. Smith, et al. and used in the work of Kuipens (2), of solving the above equation was used. This method has been completely described by Herget (3) and others (6). It will not be discussed here except to say that it does not give acceptable results when applied to spectral lines that are narrower than about three times the width of the slit function.

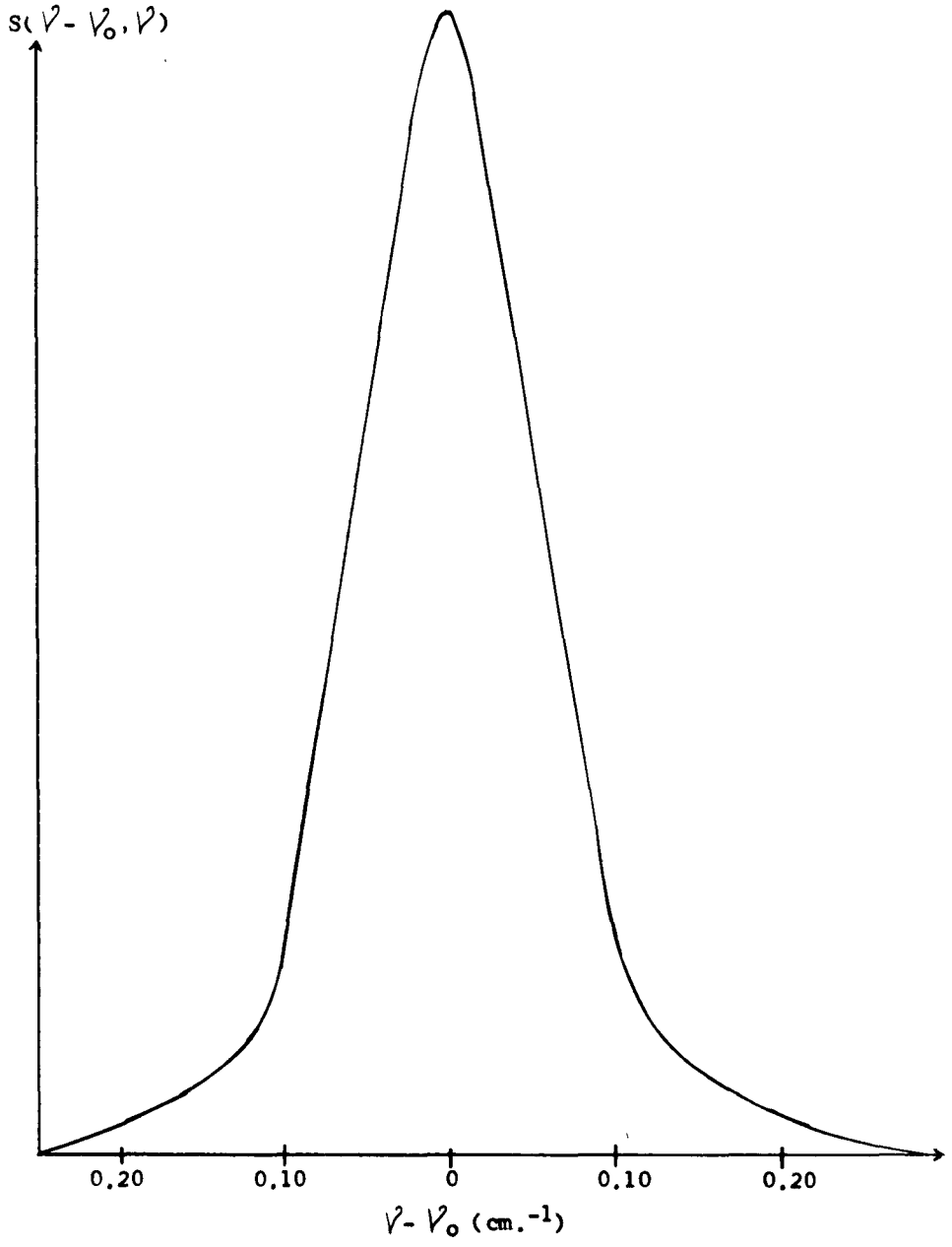

Figure 3. Slit function versus frequency difference, $\nu - \nu_0$.

TABLE II

NORMALIZED 75 μ SLIT FUNCTION: ORDINATES ARE GIVEN AT INTERVALS OF 0.02 CM^{-1}

Arbitrary Units	Normalized	Arbitrary Units	Normalized
1.1	0.0002	536.9	0.1238
3.9	0.0009	434.6	0.0990
6.7	0.0015	319.5	0.0737
9.5	0.0021	207.4	0.0478
12.5	0.0028	129.6	0.0299
15.5	0.0035	85.5	0.0170
19.4	0.0045	56.8	0.0131
28.0	0.0065	38.0	0.0088
42.5	0.0096	26.1	0.0066
65.9	0.0138	20.1	0.0048
107.8	0.0248	16.8	0.0039
207.5	0.0498	15.0	0.0030
331.0	0.0763	12.0	0.0025
449.5	0.1007	10.0	0.0020
537.5	0.1240	6.7	0.0015
593.0	0.1368	3.9	0.0009
		1.1	0.0002

CHAPTER III

RESULTS AND CONCLUSIONS

I. LINE SHAPES

The well-known expression for the shape of a Lorentz-like spectral line is

$$\alpha = \frac{\alpha_o (\Delta \nu)^2}{(\nu - \nu_o)^n + (\Delta \nu)^2} \quad , \tag{1}$$

where α is the absorption coefficient (in $cm.^{-1}$) at frequency ν (in $cm.^{-1}$), α_o is the maximum value of the absorption coefficient and is measured at the line center, ν_o. The quantity $\Delta\nu$ is the Lorentz half-width of the spectral line and is equal to $|\nu - \nu_o|$ measured where α is equal to one-half of α_o. The quantity n is the Lorentz exponent. If n is equal to 2, the line is said to be Lorentzian. If it has some value other than 2, the line is said to be non-Lorentzian.

The absorption coefficient α at a particular frequency is related to the transmission, T, at that frequency by

$$T = e^{-\alpha L} \quad , \tag{2}$$

where e is the base of the natural logarithms and L is the path length in the absorbing gas measured in cm.

It is apparent from equation (1) that it is necessary to measure α_o, $\Delta\nu$, n, and ν_o in order to determine the shape of a particular spectral line.

The lines recorded by the spectrometer were converted to per cent absorption versus frequency in $cm.^{-1}$. These data were corrected for instrumental broadening with the aid of an IBM 1620 computer according to the method discussed in Chapter II. This procedure was carried out for each line that was broad enough to be corrected. The reproducibility of the lines was checked by scanning each spectral line three or more times under the same conditions.

Per cent absorption measurements were made 0.02 $cm.^{-1}$ apart on the narrowest lines and 0.04 $cm.^{-1}$ apart on all other lines. This increment was chosen because of the limited capacity of the IBM 1620 computer.

After the lines were corrected, α was calculated from equation (2) for selected values of the frequency. This calculation was done by making use of the relation

$$T = 1 - A ,$$

where A is the absorption. Since it was not necessary to correct these lines for overlap, one then chooses the largest value of α as α_o.

The computed values of α_o are listed in Table III together with the path lengths used to determine them.

For R(10) and R(11), α_o was determined with two different path lengths. The values obtained for R(11) were in good agreement, but the values obtained for R(10) did not agree as well. This is due to the fact that in the shorter cell the per cent absorption was small enough so that a small error in determining the base or zero line would be greatly amplified in determining α_o. At less than 23 per cent or greater

TABLE III

VALUES OF α_o, $\Delta\tilde{\nu}$, AND n FOR DIFFERENT PATH LENGTHS CALCULATED BY IBM 1620 COMPUTER FROM DATA IN APPENDIX

Spectral Line	18.14 cm. path			9.78 cm. path			1.92 cm. path		
	α_o ($cm.^{-1}$)	$\Delta\tilde{\nu}$ ($cm.^{-1}$)	n	α_o ($cm.^{-1}$)	$\Delta\tilde{\nu}$ ($cm.^{-1}$)	n	α_o ($cm.^{-1}$)	$\Delta\tilde{\nu}$ ($cm.^{-1}$)	n
R(11)	0.032	0.18	1.97	0.031	0.19	2.00			
R(10)				0.145	0.24	2.01	0.135	0.26	1.97
R(9)							0.459	0.29	2.02

than 77 per cent absorption, an error of 1 per cent in determining the base or zero line would result in an error of 8 per cent in α_o. For this reason it is felt that the values obtained for α_o for R(10) in the 1.92 cm. cell is in error. The maximum per cent absorption obtained on this line was 23 per cent; however, all other values were determined with per cent absorption values ranging from 35 to 70 per cent. In this range small errors are not amplified as much.

Determination of $\Delta\nu$, n, and ν_o

The method of D. F. Smith (2) was used in the analysis of the data to determine $\Delta\nu$, n, and ν_o. The use of this method involves the rearranging of equation (1) to give

$$\frac{\alpha_o - \alpha}{\alpha} = \frac{(\nu - \nu_o)^n}{(\Delta\nu)^2} \quad . \tag{3}$$

Then from this equation two other useful equations can be obtained.

$$\left(\frac{\alpha_o - \alpha}{\alpha}\right)^{1/n} = \nu\,(\Delta\nu)^{-2/n} - \nu_o\,(\Delta\nu)^{-2/n} \tag{4}$$

and

$$\ln \frac{\alpha_o - \alpha}{\alpha} = n \ln \left|\nu - \nu_o\right| - 2 \ln (\Delta\nu) \quad . \tag{5}$$

Both equations are of the form

$$Y = mx + b \ ,$$

and therefore graphs of equations (4) and (5) should be straight lines.

If a sign factor is introduced into equation (4), and one plots

$$\left(\frac{\alpha_o - \alpha}{\alpha}\right)^{1/n} \text{(sign factor)}$$

as a function of ν, one obtains a straight line with an intercept equal to ν_o. The only advantage of using the sign factor is to reflect one leg of the "V" that would be obtained due to the change in sign of $(\nu - \nu_o)$ as ν passes through ν_o.

In the actual plot of equation (4), the sign factor used was

$$\frac{\nu - \nu_o}{|\nu - \nu_o|} ,$$

and n was assumed to be equal to 2. This is acceptable since this graph is used to determine the line center and not n. The only effect n has on the graph is to determine its slope, and this would not change the point at which the curve crosses the frequency axis. The intercept of the curve with the frequency axis determines the line center used in equation (5). As an example, Figure 4 shows the graph of equation (4) at 4 atmospheres pressure.

All line centers determined in this manner were in good agreement with line centers determined by the methods discussed in Chapter II. The reason for using the methods discussed earlier is that a spectral line must be at least broad enough to be corrected for instrumental broadening before this method can be applied, and most of the spectral lines investigated in this work at pressures less than 4 atmospheres were too narrow to be corrected.

In equation (5) one plots

$$\ln \frac{\alpha_o - \alpha}{\alpha} \qquad \text{as a function of} \quad \ln |\nu - \nu_o| .$$

This graph should also be a straight line with a slope of n. From the intercept where $\ln |\nu - \nu_o| = 0$, the Lorentz half-width can be calculated.

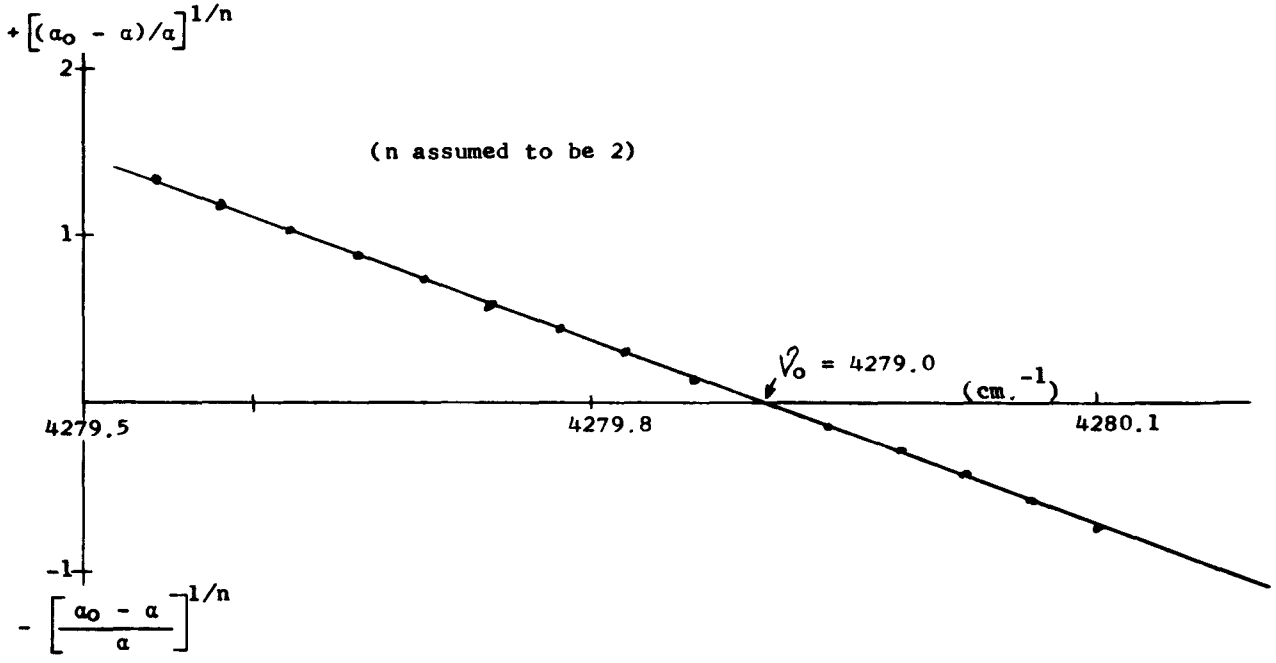

Figure 4. $\left[\frac{a_o - a}{a}\right]^{1/n}$ versus ν for R(9) at 4 atmospheres pressure.

This intercept is equal to $-2 \ln (\Delta \nu)$. Figure 6 is a graph of equation (5) for R(9) at 4 atmospheres. Graphs of these equations were made for each spectral line investigated in this work.*

It is to be noted that this method becomes inaccurate in two regions of the spectral line: first, when α approaches α_o, and second, far out in the wings of a line. In either of these positions an error in determining α produces a much larger error in $\frac{\alpha_o - \alpha}{\alpha}$. When α is less than 10 per cent or greater than 90 per cent of α_o, an error of 1 per cent in α causes an error of 12 per cent in $\frac{\alpha_o - \alpha}{\alpha}$. For this reason, only the points where the per cent absorption was between 10 and 88 per cent were used. The data used in these equations are presented in the Appendix.

The slope of the graph of equation (5) was 2, within experimental error, for each line investigated. This shows that each of these lines are truly Lorentzian in shape even at pressures of 4 atmospheres. This is in excellent agreement with Herget's work on high J lines. The actual values of n obtained for each spectral line are listed in Table III.

The values determined for the Lorentz half-width, $\Delta \nu$, are also listed in Table III along with the path length in which they were determined for each spectral line investigated. The Lorentz half-widths

---

*The values of $\ln \frac{\alpha_o - \alpha}{\alpha}$ and $\left[\frac{\alpha_o - \alpha}{\alpha}\right]^{1/n}$ were calculated with the aid of an IBM computer available at The University of Tennessee Computing Center.

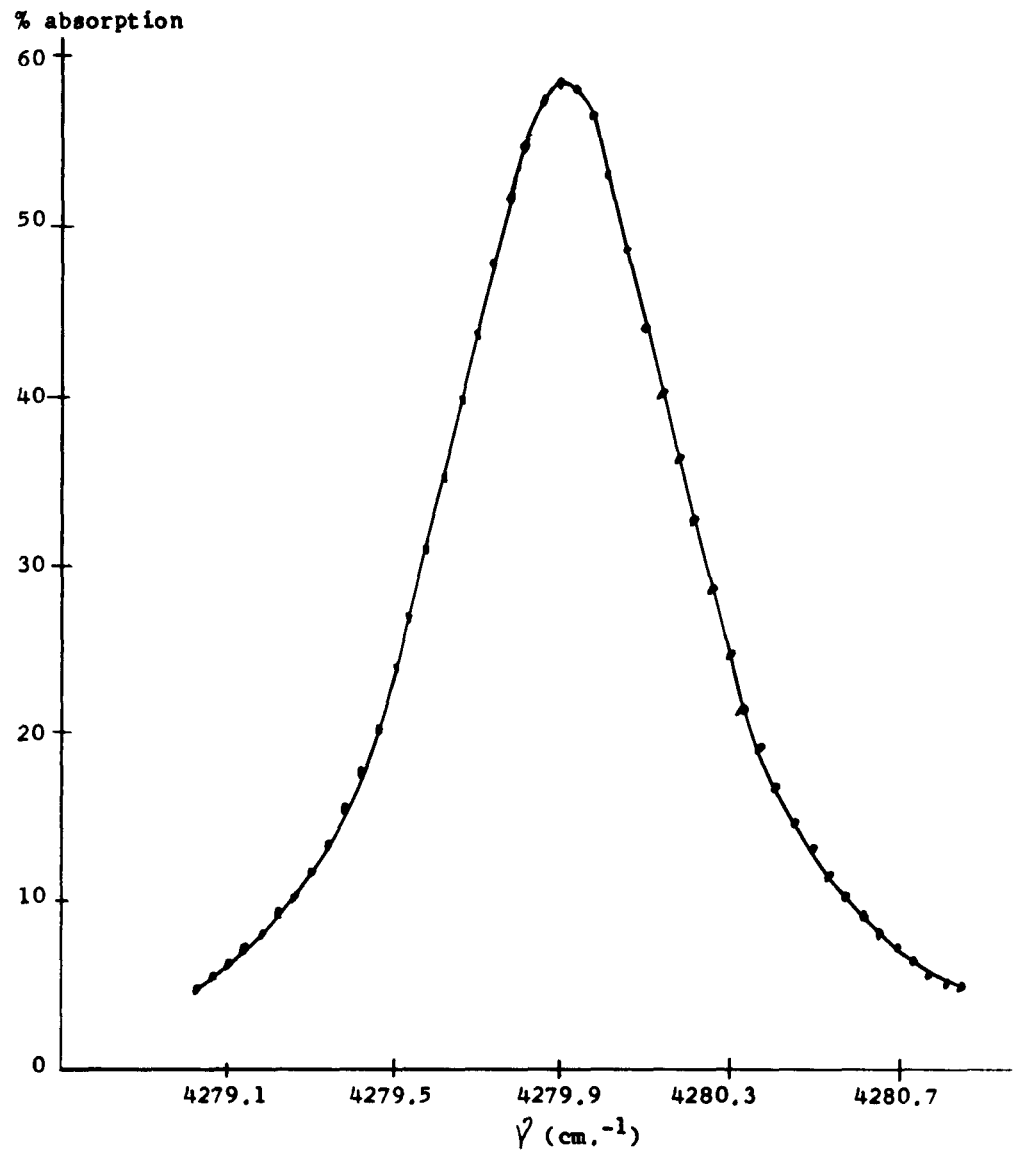

Figure 5. The observed line shape of R(9) at 4 atmospheres pressure and 100°C after correction for instrumental broadening.

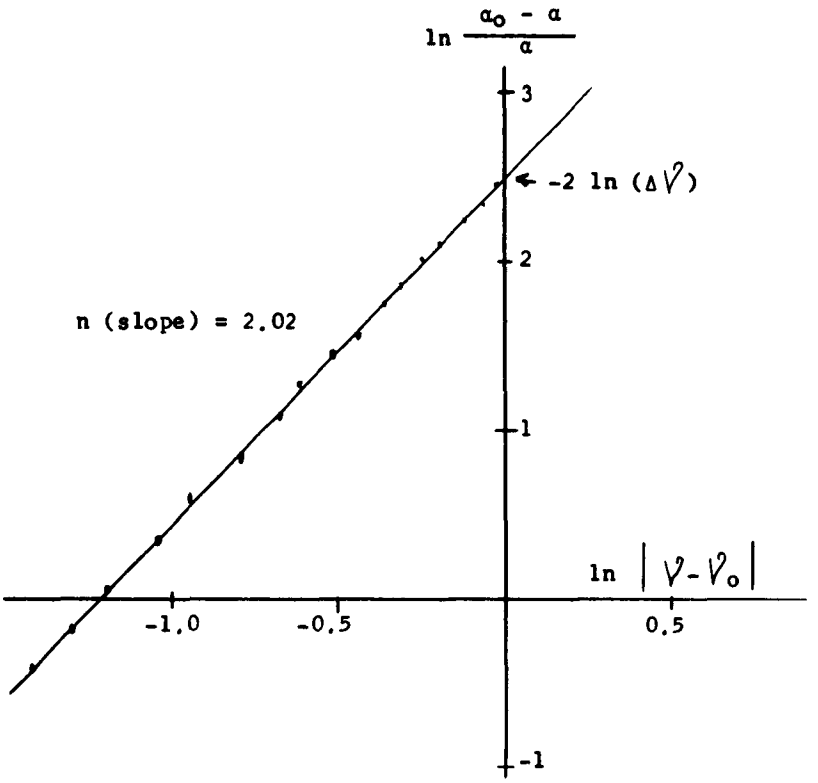

Figure 6. $\ln \frac{\alpha_o - \alpha}{\alpha}$ versus $\ln \left| \nu - \nu_o \right|$ for R(9) at 4 atmospheres pressure.

of R(10) and R(11) were determined for two different path lengths and seem to be slightly dependent on the path length. There is a possibility of an error of about 2 per cent in the pressure measurements which would produce an error of 2 per cent in the Lorentz half-width since they are directly proportional. However, this error could not account for the differences in the values of $\Delta\nu$ obtained. Thus it appears that the Lorentz half-width is slightly influenced by the path length.

Spectral lines with the same value of $|m|$ should have their Lorentz half-width proportional to pressure if they are truly Lorentzian. Thus the quantity $\frac{\Delta\nu}{P}$ would be constant for any one line at different pressures. Figure 7 shows the quantity $\frac{\Delta\nu}{P}$ plotted as a function of $|m|$. The values of $\frac{\Delta\nu}{P}$ were calculated from the data listed in Table III. All values of $\frac{\Delta\nu}{P}$ for $|m|$ less than or equal to 9 were calculated from data taken by Herget (3).

II. LINE POSITIONS

The angular positions of R(9) and R(10) used to determine K and Θ in the grating equation were measured in the 9.78 cm. cell at 50 cm. pressure. This pressure was used because the values available for the line centers had been determined at 50 cm. of pressure. Each angular position was determined four times, and agreement was within about $\pm$ 0.02 seconds of arc. At this angle this is within $\pm$ 0.02 $cm.^{-1}$.

The angular position of R(11) was determined at 10 cm. pressure in the 9.78 and 18.14 cm. cell. This angular position was determined

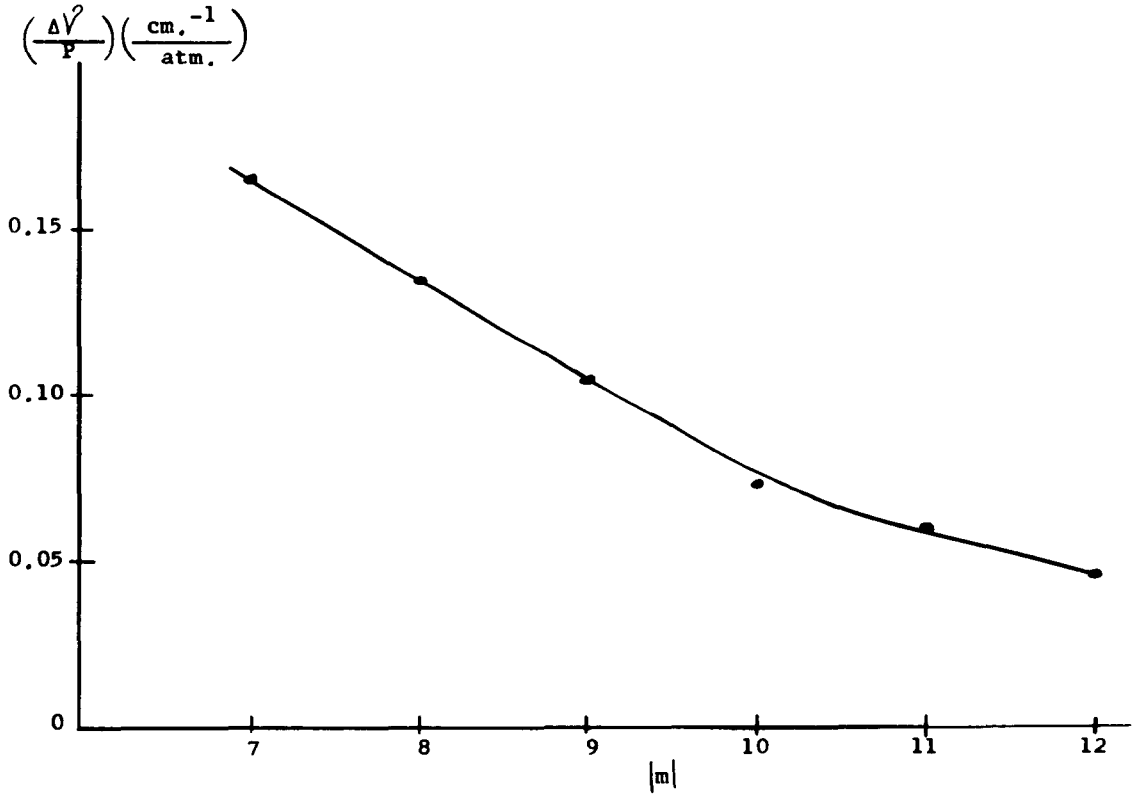

Figure 7. $\frac{\Delta V^2}{P}$ versus $|m|$ at 100°C.

six times and agreement was good. The value of the frequency for R(11) was then determined from the grating equation to be 4320.97 $cm.^{-1}$. This corresponds to a value of 4320.94 $cm.^{-1}$ calculated from the equation

$$\nu_m = \sum_{k=0}^{7} c_k m^k ,$$

where m is equal to J+1 in the R branch and c is a constant. All constants used in this calculation except c_o and c_1 were those determined by Mann and his coworkers (7) from emission spectroscopy. The values of c_o and c_1 used where those determined by Herget (3), since it was felt his values of these constants were more accurate than Mann's.

Pressure-induced line center shifts for pressures up to 5 atmospheres for each of the spectral lines investigated in this work have been examined by Herget (3). His work was at temperatures ranging from 100 to 120°C, and he found line center shifts of the order of 0.05 $cm.^{-1}$.

This investigation has in part confirmed this earlier work. No scans were made at pressures as low as 1 cm. nor with temperatures other than 100°C; however, comparison of our shift per unit pressure data shows agreement.

Table IV lists the values obtained for the line centers at 50 cm. and 4 atmospheres pressure. Each value is the average of at least three measurements. The shifts obtained per unit pressure by Herget are also listed for comparison.

TABLE IV

LINE CENTERS AND LINE SHIFTS PER UNIT PRESSURE
MEASURED AT 50 CM. AND 4 ATM.

Spectral Line	50 cm. $cm.^{-1}$	4 atm. $cm.^{-1}$	Shift/P $\frac{cm.^{-1}}{atm.}$	Shift/P[a] $\frac{cm.^{-1}}{atm.}$
R(11)	4320.97	4320.94	-0.01	-0.01
R(10)	4301.45	4301.41	-0.01	-0.01
R(9)	4279.94	4279.90	-0.01	-0.015

[a]All values in this column were calculated from data taken by Herget.

III. LINE INTENSITIES

The influence of vibration-rotation interactions on line intensities has been treated by Herman and Wallis (8) and subsequently by Herman, Rothery, and Rubin (9). The equation Herman and Wallis (8) derive for the intensity of a line in a fundamental vibration-rotation band of a diatomic molecule is

$$I_o^1(m) = \frac{8\pi^3 N_{O,J}}{3hc\,(2J+1)} \omega_o^1(m) \left|m\right| \left|R_o^1\right|^2 F_o^1(m) \qquad (7)$$

where R_o^1 is the matrix element of the electric dipole moment for a non-rotating anharmonic oscillator in the transition from ground state to the first excited state. The quantity $F_o^1(m)$ is a correction factor taking into account the interaction of vibration and rotation. In this equation h is Planck's constant, J is the quantum number of the rotational energy states, m is equal to J+1 in the R branch and -J in the P branch, c is the velocity of light, $N_{O,J}$ is the number of molecules per unit volume in the J^{th} rotational state of the ground vibrational state, and $\omega_o^1(m)$ is the frequency of the transition in $cm.^{-1}$.

The total line intensity, $I_o^1(m)$, of a spectral line can also be expressed as

$$I_o^1(m) = \int_0^\infty \alpha_m(\nu)\, d\nu \qquad (8)$$

where the absorption coefficient α and the frequency ν are expressed in $cm.^{-1}$; and $I_o^1(m)$, therefore, has the dimension $cm.^{-2}$.

If a line is truly Lorentzian, (n=2), then the value of α from equation (1) can be substituted into equation (8) and the result integrated to give

$$I_o^1(m) = \pi a_o \Delta V . \qquad (9)$$

Then by using equations (7) and (9), one can calculate the quantity $\left|R_o^1\right|^2 F_o^1(m)$ from the measured intensity and transition frequency. In order to determine $N_{O,J}$ for equation (7), one can use the relation given by Hertzberg (10)

$$N_{O,J} = \frac{N_o\ (2J+1)}{Q_v\ Q_r} \quad \exp\left[-\frac{(G+F)}{kT}\right] \qquad (10)$$

where Q_v and Q_r are the vibrational and rotational partition functions, G and F are the vibrational and rotational energies of the initial state, k is Boltzman's constant, T is the temperature (in degrees K), and N_o is the total number of molecules per unit volume. N_o can be approximated from the ideal gas law

$$P = N_o kT , \qquad (11)$$

where P is the pressure.

In this manner $\left|R_o^1\right|^2 F_o^1(m)$ has been calculated for each HF line investigated. Lovell, et al. (11) have calculated this quantity for all HF lines between P(6) and R(7). A plot of $\left|R_o^1\right|^2 F_o^1(m)$ versus $|m|$ is shown in Figure 8 for all values calculated by the author or by Lovell.

The intersection of a curve drawn through these points with the m=0 curve will yield a value for $\left|R_o^1\right|^2$ since $F_o^1(0) = 1$. The value obtained for $\left|R_o^1\right|^2$ by Lovell was 0.97×10^{-38} esu^2 cm.^{2}.

Then by using this value of $\left|R_o^1\right|^2$ one can determine the rotational correction factor $F_o^1(m)$. The rotational correction factor, $F_o^1(m)$, obtained experimentally are compared in Figure 9 with those calculated by Herman, et al. (9) for a rotating Morse or Pekeris oscillator. All values

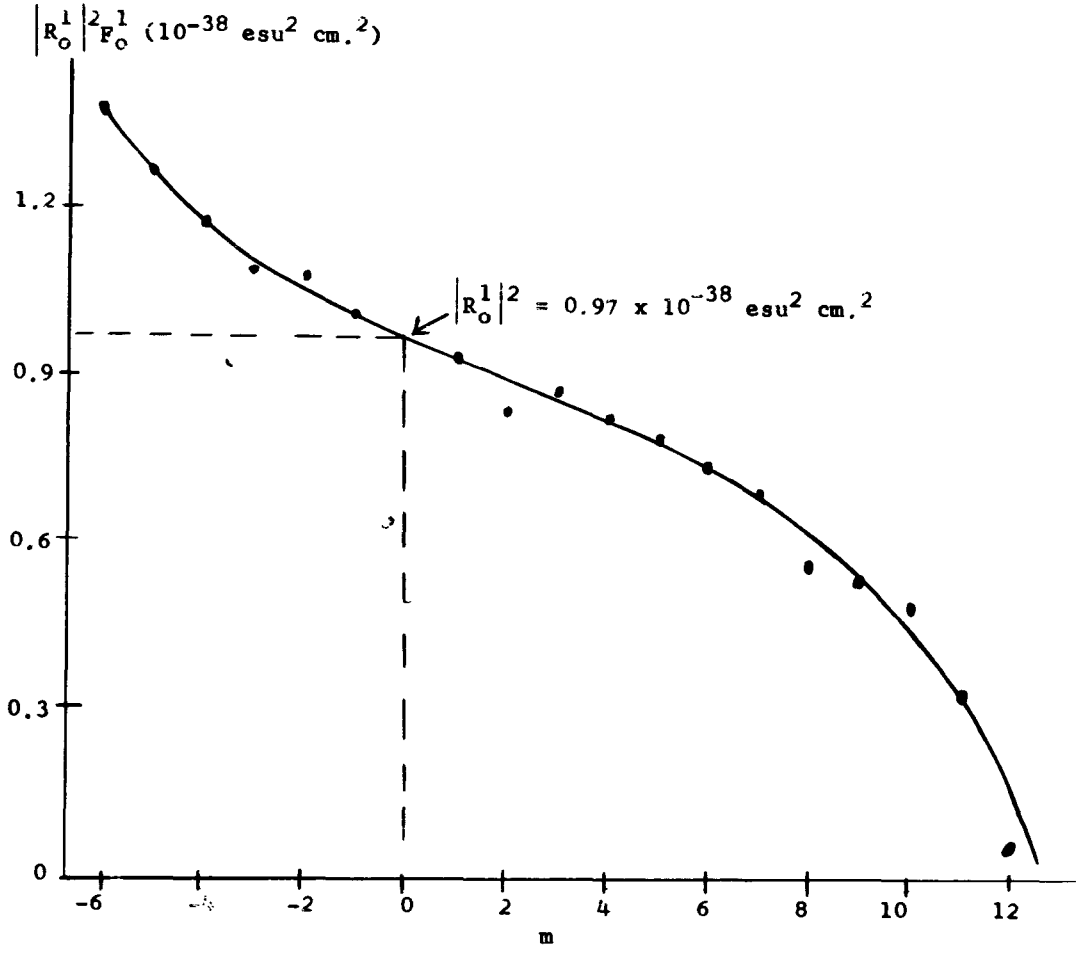

Figure 8. $|R_o^1|^2 F_o^1(m)$ versus m.

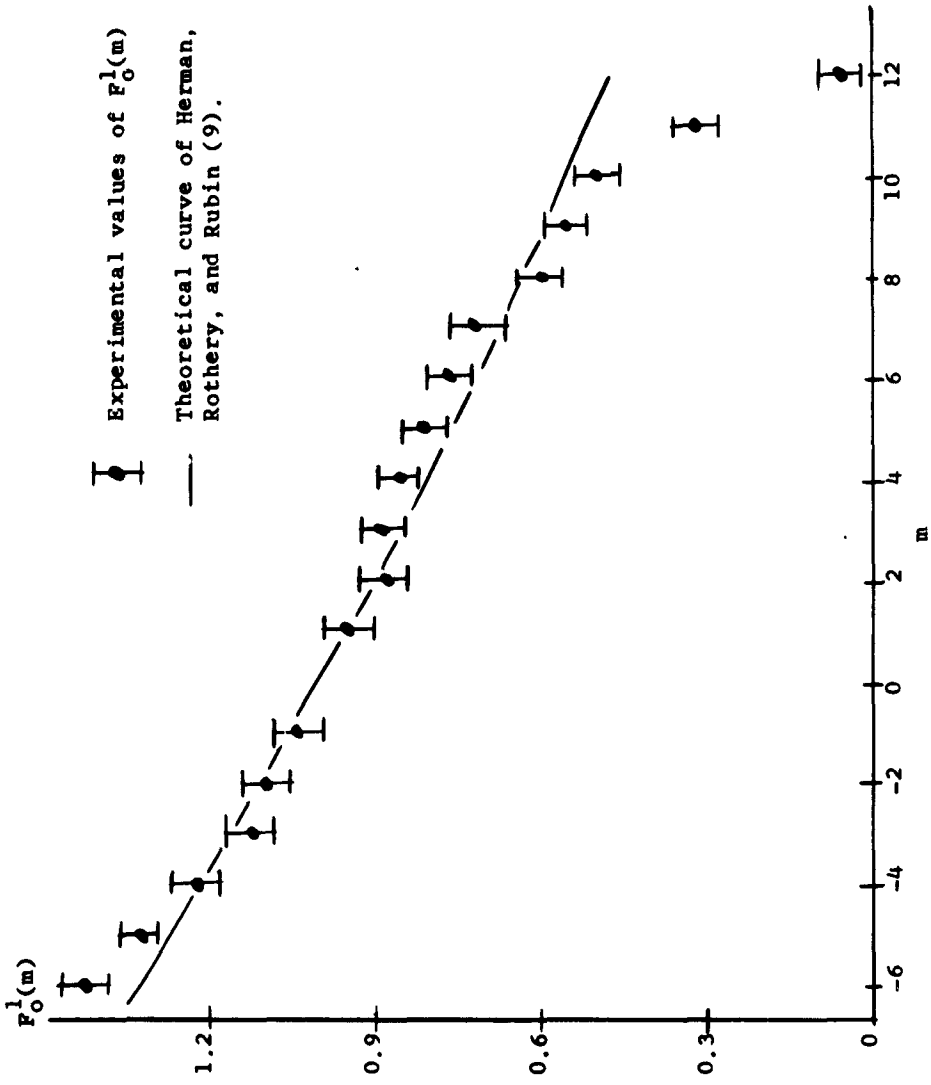

Figure 9. $F_o^1(m)$ versus m.

of $F_0^1(m)$ between m= -6 and m=8 are those determined by Lovell. The value of $F_0^1(m)$ for m=9 was calculated from data taken earlier by Herget (3).

The theoretical expression of Herman et al. (9) requires the use of the experimental value of the interaction constant Θ. Error in the value of this constant depends primarily on the intensity of the spectral lines with m= $\pm$1 or $\pm$2. It has been estimated by Lovell that the error in the value of Θ is about $\pm$ 3 per cent. This error would change the value of $F_0^1(m)$ by about $\pm$ 0.01 in the theoretical expression. The experimental values of $F_0^1(m)$ in Figure 9 are shown with their estimated error.

The reasonably close fit of the theoretical curve to the experimental values of $F_0^1(m)$ for $|m|$ less than 8 appears to indicate that a Pekeris oscillator is a fair approximation to the HF molecule for small J. For high J there is a disagreement between theory and experiment. With due regard for the fact that the $F_0^1(m)$ are not as accurate for large m as for small m, it does appear that the $F_0^1(m)$ curve is S-shaped.

Table V is a list of $I_0^1(m)$, $|R_0^1|^2 F_0^1(m)$, and $F_0^1(m)$ determined in this work. All values for m=9 were determined from earlier data taken by Herget (3).

TABLE V

MEASURED VALUES OF $I_o^1(m)$, $\left|R_o^1\right|^2 F_o^1(m)$, AND $F_o^1(m)$

m	$I_o^1(m)$ (cm.$^{-1}$/atm.)	$\left\|R_o^1\right\|^2 F_o^1(m)$ (10^{-38} esu^2 cm.^{2})	$F_o^1(m)$
9	0.415	0.53	0.55
10	0.105	0.47	0.49
11	0.026	0.31	0.32
12	0.005	0.05	0.05

CHAPTER IV

SUMMARY AND SUGGESTIONS FOR FUTURE WORK

I. SUMMARY

The aim of this investigation was to determine experimentally the true line shape and line position for as many as possible of the high J rotational absorption lines in the hydrogen fluoride fundamental band. The line shapes were to be determined at identical temperatures and at pressures where pressure broadening made the only significant contribution to the line shape.

All data were taken on the high resolution vacuum-grating spectrometer at The University of Tennessee. The HF lines were used as internal standards for calibrating purposes. The R(5) line of the first overtone of CO was used to determine the slit function to correct measured line shapes for distortions caused by instrumental broadening.

The line position of R(11) was measured to be 4320.97 $cm.^{-1}$. This agrees to within 0.03 $cm.^{-1}$ with the calculated value.

The line shapes of R(9), R(10), and R(11) were determined and found to be truly Lorentzian. α_o and $\Delta\nu$ were determined for R(10) and R(11) in two different path lengths. The α_o's agreed within experimental error, but the $\Delta\nu$'s seemed to be slightly dependent on the path length.

The intensities of these lines were measured and the rotational correction factors, $F_o^1(m)$, determined. The rotational correctional factors were found to disagree with those predicted theoretically by Herman et al. (9).

Pressure-induced shifts in the centers of the high J rotational lines investigated were measured and found to agree with earlier measurements by Herget (3).

II. SUGGESTIONS FOR FUTURE WORK

1. Measure the temperature dependence of the parameters describing the shape of a spectral line.

2. Measure the high J line shape and intensity in the P branch of the fundamental band. This could be accomplished with the aid of a cooled lead sulfide detector, and present equipment. Indications from this present work and the work done by Herget and Lovell (11) are the intensity of these lines would be greatly enhanced, because of the increase in the rotational correctional factor in this region.

3. Measure the Lorentz half-width for several lines, say R(7) and R(8), in two or more path lengths. These lines would be broad enough to correct for instrumental broadening at pressures where overlapping of neighboring lines would not be a problem. The different path lengths could be made from one cell similar to the 1.92 cm. cell used in this work by reaming out the window seat and replacing it with spacers of different thickness.

4. Measure the line position, shape, and intensity for more of the high J lines in the R branch. This could be accomplished by using a cell of a few meters path length. The information from such measurements would permit a better determination of the smaller rotational constants than now exists and provide a further check on the trend of the rotational correction factors.

BIBLIOGRAPHY

BIBLIOGRAPHY

1. Kuipers, G. A., "The Spectrum of Monomeric HF: Molecular Constants, Line Shapes, Intensities, and Breadths," Ph. D. Thesis, Department of Physics, University of Tennessee (June 1956).

2. Smith, D. F., J. Mol. Spectroscopy 3, 473 (1959).

3. Herget, W. F., "The Infrared Spectrum of Hydrogen Fluoride: Line Positions and Line Shapes," Ph. D. Thesis, Department of Physics, University of Tennessee (June 1962).

4. Private communication with the author.

5. Herndon, J. A. and A. H. Nielsen, "Design and construction of a Vacuum-Grating Spectrometer for the Infrared," Technical Report No. 2, Office of Ordinance Research, Department of the Army (December 1957).

6. Deeds, W. E., N. M. Gailar, W. F. Herget, T. M. Holladay, R. J. Lovell, A. A. Mason, and A. H. Nielsen, "Line Intensities and Pressure Broadening Studies in HF," Air Force Cambridge Research Laboratories Report No. 465 (March 1961).

7. Mann, D. E., B. A. Thrush, D. R. Lide, Jr., J. J. Ball, and N. Acquista, J. Chem. Phys. 34, 420 (1961).

8. Herman, R., and R. F. Wallis, J. Chem. Phys. 23, 637 (1955).

9. Herman, R., R. W. Rothery, and R. J. Rubin, J. Mol. Spectroscopy 2, 369 (1958).

10. Hertzberg, G., Spectra of Diatomic Molecules (D. Van Nostrand Co., Inc., New York, 1953).

11. Lovell, R. J., and W. F. Herget, J. Optical Society,(to be published December 1962).

APPENDIX

TABLE VI

SPECTRAL LINE SHAPES IN TERMS OF α AND $\nu - \nu_0$ FOR LINES MEASURED AT 4 ATM. PRESSURE AND 100°C

Spectral Line Cell Length	$\nu - \nu_0$ ($cm.^{-1}$)	α Low Side ($cm.^{-1}$)	α High Side ($cm.^{-1}$)
R(9)			
1.92 cm. cell	0.04	0.447	0.455
	0.08	0.410	0.432
	0.12	0.379	0.392
	0.16	0.340	0.346
	0.20	0.301	0.301
	0.24	0.262	0.266
	0.28	0.226	0.234
	0.32	0.186	0.206
	0.36	0.162	0.174
	0.40	0.138	0.145
	0.44	0.118	0.123
	0.48	0.102	0.110
	0.52	0.088	0.097
	0.56	0.074	0.089
	0.60	0.063	0.078
	0.64	0.055	0.065
	0.68	0.049	0.057
	0.72	0.043	0.050
	0.76	0.039	0.044
	0.80	0.035	0.040
R(10)			
9.78 cm. cell	0.04	0.135	0.138
	0.08	0.118	0.123
	0.12	0.099	0.107
	0.16	0.083	0.093
	0.20	0.071	0.082
	0.24	0.062	0.072
	0.28	0.053	0.061
	0.32	0.046	0.051
	0.36	0.038	0.042
	0.40	0.032	0.035
	0.44	0.026	0.029
	0.48	0.023	0.025
	0.52	0.021	0.022
	0.56	0.019	0.020
	0.60	0.018	0.017
	0.64	0.016	0.015
	0.68	0.014	0.013
	0.72	0.012	0.011

TABLE VI (CONTINUED)

Spectral Line Cell Length	$\nu - \nu_o$ ($cm.^{-1}$)	α Low Side ($cm.^{-1}$)	α High Side ($cm.^{-1}$)
R(10)			
1.92 cm. cell	0.02	0.132	0.130
	0.04	0.130	0.128
	0.06	0.126	0.122
	0.08	0.120	0.116
	0.10	0.112	0.108
	0.12	0.105	0.100
	0.14	0.098	0.094
	0.16	0.091	0.087
	0.18	0.085	0.082
	0.20	0.078	0.076
	0.22	0.072	0.071
	0.24	0.066	0.066
	0.26	0.060	0.059
	0.28	0.055	0.053
	0.30	0.049	0.047
	0.32	0.043	0.043
	0.34	0.038	0.038
	0.36	0.032	0.035
	0.38	0.028	0.031
	0.40	0.025	0.029
	0.42	0.022	0.027
R(11)			
9.78 cm. cell	0.02	0.030	0.031
	0.04	0.029	0.029
	0.06	0.027	0.026
	0.08	0.025	0.024
	0.10	0.023	0.022
	0.12	0.021	0.020
	0.14	0.020	0.018
	0.16	0.018	0.017
	0.18	0.017	0.015
	0.20	0.015	0.014
	0.22	0.014	0.012
	0.24	0.012	0.011
	0.26	0.011	0.010
	0.28	0.010	0.008
	0.30	0.008	0.007
	0.32	0.007	0.006
	0.34	0.006	0.005
	0.36	0.005	0.004

TABLE VI (CONTINUED)

Spectral Line Cell Length	$\nu - \nu_o$ ($cm.^{-1}$)	α Low Side ($cm.^{-1}$)	α High Side ($cm.^{-1}$)
R(11)			
18.14 cell	0.02	0.031	0.031
	0.04	0.030	0.029
	0.06	0.028	0.026
	0.08	0.026	0.023
	0.10	0.024	0.021
	0.12	0.022	0.019
	0.14	0.020	0.017
	0.16	0.018	0.015
	0.18	0.017	0.014
	0.20	0.015	0.012
	0.22	0.013	0.011
	0.24	0.012	0.010
	0.26	0.010	0.009
	0.28	0.009	0.008
	0.30	0.008	0.007
	0.32	0.007	0.006
	0.34	0.006	0.006
	0.36	0.005	0.005
	0.38	0.004	0.005
	0.40	0.004	0.004
	0.42	0.003	0.004

Distribution List G-A

Code	Organization	No. Copies
1-1	Science Advisor Department of State Washington 25, D. C. (U)	1
1-6	Office of Secretary of Defense (DDR&E, Tech. Library) Washington 25, D. C. (U)	1
2-2	Institute of Technology Library MCLI-LIB, Bldg. 125, Area B Wright-Patterson Air Force Base, Ohio	1
2-4	Hq. USAF (AFCSA, Secretary) Washington 25, D. C.	1
2-8	AFCRL, OAR (CRIPA) Stop 39 L. G. Hanscom Field Bedford, Massachusetts	20
2-9	ARL (ARA-2) Library AFL 2292, Building 450 Wright-Patterson AFB, Ohio	1
2-10	ESD (ESRDG) L. G. Hanscom Field Bedford, Massachusetts	1
2-14	ASD (ASAPRD-Dist) Wright Patterson AFB, Ohio	1
2-16	ACIC (ACDEL-7) 2nd & Arsenal St. Louis 18, Missouri (U)	1
2-19	NAFEC Library Branch, Bldg. 3 Atlantic City, New Jersey Attn: RD-702	1
2-107	AWS (AWSSS/SIPD) Scott AFB, Illinois	1
2-119	A. U. (Library) Maxwell AFB, Alabama	1
3-8	Dept. of the Army (SIGRD-8-B-5) Washington 25, D.C.	1
3-9	Technical Documents Center Evans Signal Labs. Belmar, New Jersey	1
2-6	Hq. USAF (AFRDR) Washington 25, D. C.	1

Code	Organization	No. of Copies
4-20	Technical Reports Librarian U. S. Naval Postgraduate School Monterey, California (U)	1
4-25	Director, U.S.Naval Res. Laboratory Code 2027 Washington 25, D. C.	1
4-41	ONR (Geophysics Code N-416) Office of Naval Research Washington 25, D. C.	1
5-9	Documents Expediting Project (UNIT X) Library of Congress Washington 25, D. C. (U)	1
5-14	Superintendent of Documents Government Printing Office Washington 25, D. C. (U)	1
5-65	ASTIA (TIPAA) Arlington Hall Station Arlington, 12, Virginia	10
5-18	National Research Council 2101 Constitution Avenue Washington 25, D. C. (U)	1
5-23	NASA; Attn: Library, Code AFET-LA Stop 85 Washington 25, D. C.	1
5-26	Librarian, Boulder Laboratories National Bureau of Standards Boulder, Colorado (U)	1
5-28	Library National Bureau of Standards Washington 25, D. C. (U)	1
5-46	Director of Meteorological Research U. S. Weather Bureau Washington 25, D. C. (U)	1
5-53	Library, U.S. Weather Bureau Suitland, Maryland (U)	1
6-87	Director, USAF Project RAND The Rand Corporation 1700 Main Street, Santa Monica, California Through: A. F. Liaison Office	1
6-90	Dr. William W. Kellogg Rand Corporation 1700 Main St., Santa Monica, California (U)	1

Code	Organization	No. of Copies
7-8	Mr. Malcolm Rigby American Meteorological Society P. O. Box 1736, Washington 13, D.C. (U)	1
7-35	Institute of Aerospace Sciences, Inc. 2 East 64th Street New York 21, New York (U)	1
8-5	Library, Geophysical Institute University of Alaska P.O. Box 938; College, Alaska (U)	1
8-41	Dr. Joseph Kaplan Dept. of Physics University of California Los Angeles, California (U)	1
8-47	Professor Fred L. Whipple Harvard College Observatory 60 Garden Street Cambridge 38, Massachusetts (U)	1
8-48	Dr. David Fultz Dept. of Geophysical Sciences University of Chicago Chicago 37, Illinois (U)	1
8-365	Dr. A. M. Peterson Stanford University Stanford, California (U)	1
8-366	Professor Clarence Palmer Institute of Geophysics University of California Los Angeles 24, California (U)	1
9-6	Technical Information Office European Office, Aerospace Research Shell Building, 47 Cantersteen Brussels, Belgium (U)	1
2-33	AFCRL, OAR (CRIP, John R. Marple) L. G. Hanscom Field Bedford, Massachusetts	1
	Remaining copies to Hq. AFCRL-OAR (CRZCI, John Garing) L. G. Hanscom Field Bedford, Massachusetts	

Air Force Cambridge Research Laboratories, Bedford, Mass. Geophysics Research Directorate.

INFRARED SPECTRUM OF HYDROGEN FLUORIDE: SHAPES, POSITIONS AND INTENSITIES OF HIGH J LINES IN THE FUNDAMENTAL BAND, by Eldreth and Lovell, December 1962. 49 pages.

AFCRL-62-1090 Unclassified Report

This report extends to lines m = −6 to m = +12 the study in the fundamental band of HF of the comparison between the theoretically predicted and experimentally determined rotational correction factors, $F_0^1(m)$. The trend of the experimental points from m = +8 to m = +12 is for an increasingly sharp drop below predicted values.

UNCLASSIFIED

Physics

Infrared Spectroscopy

Eldreth, L. F. and Lovell, R. J.

UNCLASSIFIED

Air Force Cambridge Research Laboratories, Bedford, Mass. Geophysics Research Directorate.

INFRARED SPECTRUM OF HYDROGEN FLUORIDE: SHAPES, POSITIONS AND INTENSITIES OF HIGH J LINES IN THE FUNDAMENTAL BAND, by Eldreth and Lovell, December 1962. 49 pages.

AFCRL-62-1090 Unclassified Report

This report extends to lines m = −6 to m = +12 the study in the fundamental band of HF of the comparison between the theoretically predicted and experimentally determined rotational correction factors, $F_0^1(m)$. The trend of the experimental points from m = +8 to m = +12 is for an increasingly sharp drop below predicted values.

UNCLASSIFIED

Physics

Infrared Spectroscopy

Eldreth, L. F., and Lovell, R. J.

UNCLASSIFIED